Title

Polycationic Open-Shell Cyclophanes: Synthesis of Electron-Rich Chiral Macrocycles, and Redox-Dependent Electronic States

Authors

Shi, Yafei

Li, Chenglong

Di, Jiaqi

et al.

Publication Date

2024-02-27

DOI

10.1002/anie.202402800

Peer reviewed

Angewandte Chemie

Eine Zeitschrift der Gesellschaft Deutscher Chemiker

www.angewandte.de

Akzeptierter Artikel

Titel: Polycationic Open-Shell Cyclophanes: Synthesis of Electron-Rich Chiral Macrocycles, and Redox-Dependent Electronic States

Autoren: Yafei Shi, Chenglong Li, Jiaqi Di, Yuting Xue, Yawei Jia, Jiaxian Duan, Xiaoyu Hu, Yu Tian, Yanqiu Li, Cuiping Sun, Niu Zhang, Yan Xiong, Tianyun Jin, and Pangkuan Chen

Zitierweise: *Angew. Chem. Int. Ed.* **2024**, e202402800

Link zur VoR: https://doi.org/10.1002/anie.202402800

WILEY VCH

10.1002/ange.202402800

WILEY-VCH

RESEARCH ARTICLE

Polycationic Open-Shell Cyclophanes: Synthesis of Electron-Rich Chiral Macrocycles, and Redox-Dependent Electronic States

Yafei Shi,[a] Chenglong Li,*[a] Jiaqi Di,[a] Yuting Xue,[a] Yawei Jia,[a] Jiaxian Duan,[a] Xiaoyu Hu,[a] Yu Tian,[a] Yanqiu Li,[a] Cuiping Sun,[a] Niu Zhang,[b] Yan Xiong,[b] Tianyun Jin,*[c] and Pangkuan Chen*[a]

[a] Y. Shi, Dr. C. Li, J. Di, Y. Xue, Y. Jia, J. Duan, X. Hu, Y. Tian, Y. Li, C. Sun and Prof. Dr. P. Chen
Beijing Key Laboratory of Photoelectronic/Electrophotonic Conversion Materials, Key Laboratory of Medical Molecule Science and Pharmaceutical Engineering of the Ministry of Industry and Information Technology, School of Chemistry and Chemical Engineering, Beijing Institute of Technology, Beijing, 102488 (China)
E-mail: pangkuan@bit.edu.cn
[b] Dr. N. Zhang and Dr. Y. Xiong
Analysis and Testing Centre, Beijing Institute of Technology
[c] Dr. T. Jin
Center of Marine Biotechnology and Biomedicine, Scripps Institution of Oceanography University of California, San Diego La Jolla, 92093, USA
E-mail: t2jin@ucsd.edu

Supporting information for this article is given via a link at the end of the document.

Abstract: π-Conjugated chiral nanorings with intriguing electronic structures and chiroptical properties have attracted considerable interests in synthetic chemistry and materials science. We present the design principles to access new chiral macrocycles (**1** and **2**) that are essentially built on the key components of main-group electron-donating carbazolyl moieties or the π-expanded aza[7]helicenes. Both macrocycles show the unique molecular conformations with a (*quasi*) figure-of-eight topology as a result of the conjugation patterns of 2,2',7,7'-spirobifluorenyl in **1** and triarylamine-coupled aza[7]helicene-based building blocks in **2**. This electronic nature of redox-active, carbazole-rich backbones enabled these macrocycles to be readily oxidized chemically and electrochemically, leading to the sequential production of a series of positively charged polycationic open-shell cyclophanes. Their redox-dependent electronic states of the resulting multispin polyradicals have been characterized by VT-ESR, UV−vis−NIR absorption and spectroelectrochemical measurements. The singlet ($\Delta E_{S\text{-}T}$ = –1.29 kcal mol^{-1}) and a nearly degenerate singlet-triplet ground state ($\Delta E_{S\text{-}T(calcd)}$ = –0.15 kcal mol^{-1} and $\Delta E_{S\text{-}T(exp)}$ = 0.01 kcal mol^{-1}) were proved for diradical dications $\mathbf{1}^{2+2\bullet}$ and $\mathbf{2}^{2+2\bullet}$, respectively. Our work provides an experimental proof for the construction of electron-donating new chiral nanorings, and more importantly for highly charged polyradicals with potential applications in chirospintronics and organic conductors.

Introduction

Studies of π-conjugated chiral macrocycles have remained one of the spotlights in synthetic chemistry over recent years because the unique nanostructured aromatic π-systems are of fundamental and technological significance with applications in supramolecular chemistry and material science.[1,2] Related architectures for early type of these systems were experimentally demonstrated in planar chiral macrocycles, which has thereby kindled increasing interests and entailed new approaches to expand this emerging area.[3] Some of the design principles established hitherto also encompass the construction of figure-of-eight cyclic conformations,[4] topological cycles[5] and several nanobelt-shaped infinitenes[6] as well as the predeterminate chiral loops with stereogenic elements embedded in π-skeletons.[7] Interestingly, those previously reported chiral macrocycles in the literature are nearly closed-shell aromatic hydrocarbons, while the macrocyclic open-shell chiral analogues are still lacking. This would substantially curtail further investigations of the spin-correlated properties in particular, for example, the electric conductivity and organic (anti)ferromagnetism.[8,9]

Organic open-shell radicals with unpaired electrons enable the modulation of spin-spin interactions which however is impossible to replicate in closed-shell species. Several main pathways have usually been traced to access neutral or charged radicals: i) diradicaloids derived from the shifted resonant structures of Thiele's and Tschitschibabin's hydrocarbon derivatives; ii) (electro)chemical oxidation-induced N/O/S-based cationic radicals, and iii) Brönsted/Lewis acid-induced radical ion pairs via intramolecular electron transfer strategy.[10-14] Introduction of main-group elements to the heteroatom-doped π-systems resulted not only in redox-active paramagnetic spins but also, more generally, in modified electronic structures with tunable optoelectronic properties as compared with the similar all-carbon-based aromatic compounds.[15-18] Furthermore, thus formed positively charged species with highly polar bonds regardless of closed or open-shell characters are expected to display unique arrangements for assembled superstructures as well as oxidation-state-dependent magnetic behaviors.[12,13] Numerous N-centered cationic radicals were successfully developed by Rajca, Wu, Wang and others in the open-chain or three-dimensional (3D) π-conjugated cage structures,[19] and several intriguing triangular trisradicals that show doublet ground states or spin frustration due to Jahn-Teller distortion have also been unraveled.[20] However, none of the known chiral macrocycles has been reported with multiple radical centers and polycationic charges.

We have recently characterized a double aza[7]helicene with redox-induced switchable aromaticity,[21] and the synthesis of a NIR-emissive π-conjugated chiral organoborane macrocycle was also described in our group.[22] Herein, we present the synthesis of two new chiral macrocycles, **1** and **2**, both of which are highly electron-rich in nature. Two units of the carbazolyl trimers are crosslinked together by the 2,2',7,7'-spirobifluorenyl fragment

10.1002/ange.202402800

WILEY-VCH

RESEARCH ARTICLE

2,2',7,7'-Spirobifluorenyl-Based Figure-of-Eight Chiral Macrocycle and Redox-Dependent Polyradical Cation Species

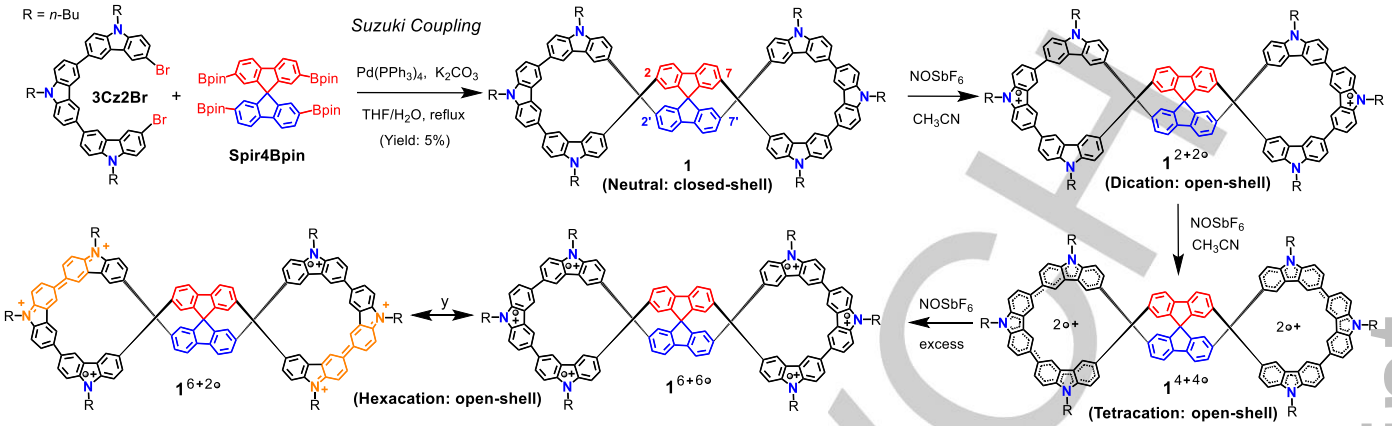

Scheme 1. Synthetic route of **1** and the formation of polyradical cationic cyclophanes with different oxidation states by redox chemistry.

Aza[7]helicene-Containing *Quasi*-Figure-of-Eight Chiral Macrocycle and Oxidation-Induced Polyradical Cations

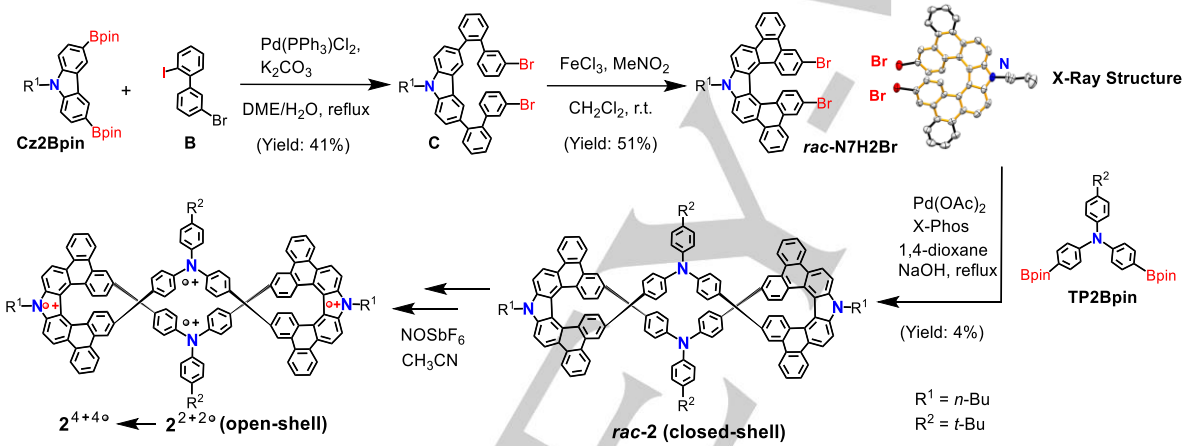

Scheme 2. Synthetic route of **2** and the formation of polyradical cationic cyclophanes by redox chemistry.

to achieve molecular chirality in the figure-of-eight macrocycle **1**. Aza[7]helicenes that are featuring the *ortho*-fused carbazole derivatives are stitched by the electron-donating triphenylamine, giving rise to a *quasi* figure-of-eight topology of **2** with a strong emission (Φ_{FL}= 0.99) and a high value of the circularly polarized luminescence (CPL) brightness (B_{CPL} = 100.2 $M^{-1}cm^{-1}$). More interestingly, these newly obtained compounds revealed robust redox-active behaviors under chemically and electrochemically controlled oxidation conditions, leading to the well-defined multispin polycationic chiral cyclophanes with the open-shell characters. Their redox-dependent electronic states were fully explored by computations, electron spin resonance (ESR) measurements, UV-vis-NIR absorption spectroscopy and spectroelectrochemical techniques. The electronic and magnetic characteristics of the current highly charged cyclophanes, however, are rarely accessible in the all-carbon-based analogues.

Results and Discussion

The synthesis of **1** was performed through the palladium-catalyzed Suzuki C-C coupling reactions as shown in **Scheme 1** and Supporting information. Reaction of the commercially available tetrabrominated 2,2',7,7'-spirobifluorenyl (**Spir4Br**) with 4 equiv of bis(pinacolate)diboron gave an conversion to tetra-boronesterified 2,2',7,7'-spirobifluorenyl (**Spir4Bpin**) as the intermediate (yield 92%). The other key precursor of the linear carbazolyl trimer (**3Cz2Br**) was obtained in 66% yield by reacting 3,6-dibromocarbazole with boronesterified carbazole (**Cz2Bpin**). Subsequently, **3Cz2Br** and **Spir4Bpin** were refluxed in THF/H_2O (v/v 5:1) with the 2:1 molar ratio, and afforded the chiral macrocycle ***rac*-1** in 5%. For the synthesis of **2**, a similar strategy was applied (Scheme 2 and SI). The coupling reaction between **Cz2Bpin** and a bifuctional known compound of bromoiodobiphenyl **(B)** gave rise to the π-extended carbazole derivative **C**, which was followed by an intramolecular dehydrogenative oxidation through Scholl reaction using $FeCl_3$ and $MeNO_2$ in CH_2Cl_2 at room temperature, leading to the *ortho*-fused aza-[7]helicene fragment ***rac*-N7H2Br** (yield 51%). Two of these brominated chiral building blocks were further coupled by 2 equiv of triarylamine donors (**TP2Bpin**) to form the *quasi* figure-of-eight chiral macrocycle ***rac*-2** in 4% yield.

Standard reaction workup procedures followed by purification via preparative column chromatography gave the cyclic products, and they were fully characterized through ^1H, ^{13}C NMR spectroscopy and were assigned with assistance of the 2D ^1H-^1H COSY NMR technique (Figure S12 and S13). Figure 1a shows

10.1002/ange.202402800

RESEARCH ARTICLE

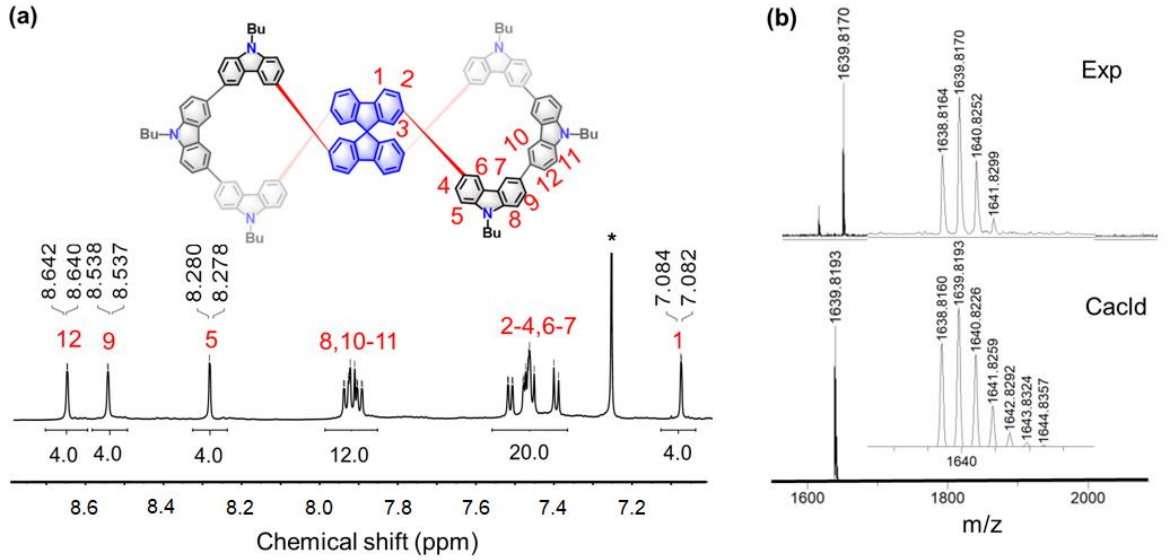

Figure 1. (a) ^{1}H NMR spectrum of **1** in the aromatic region (700 MHz, $CDCl_3$, r.t., the asterisk indicates $CDCl_3$). (b) MALDI-TOF mass spectrum (positive-ion mode) of **1** showing experimental and simulated isotopic patterns.

four doublet resonances that are slightly overlapped in the aromatic region of ^{1}H NMR spectrum ($CDCl_3$, 25 °C, Figure S10), and they can be assigned to H_1, H_5, H_9 and H_{12} from the two sets of carbazole units and one type of fluorene in **1**. All the other signals corresponding to the macrocyclic structure are considerably overlapped. The formation of **1** and **2** was further confirmed by high-resolution MALDI-TOF-MS, in which the major peak was observed at *m/z* 1639.8170 and 1641.7670, respectively, corresponding to the molecular ion (calcd 1639.8193 for **1** and 1641.7663 for **2**) (Figure 1b; others are shown in SI).

The optical resolution of **1** and **2** were performed via the preparative chiral high-performance liquid chromatography (HPLC) on Daicel Chiralpak IA-3 and IG-3 column under ambient conditions, respectively (Figures S46 and S47). Both stereoisomers (**1**-P/**1**-M and **2**-PP/**2**-MM) were sufficiently isolated, leading to a high enantiomeric excess (>99% *ee*, Table S7). No diastereoisomer (i.e. the mesomer **2**-PM) was detected in the macrocyclization reaction of **2**. A considerably high racemization barrier $\Delta G^{\ddagger}$ = 63.6 kcal/mol was calculated for **2** (Figures S58 and S59), according to the proposed isomerization from **2**-MM to *meso* **2**-PM through a transition state (TS) with the two extremities of aza[7]helicene oriented face-to-face and confirmed by the intrinsic reaction coordinate (IRC) calculations (B3LYP/6-31G*). The temperature-dependent *ee* values of the enantiomeric **2**-PP were experimentally monitored by HPLC in 1,3,5-triisopropyl-benzene but without an increase of the other enantiomer observed with the *ee* values maintained > 99% after a thermal treatment up to 200 °C for 3 h (Figure S53). The possibility to racemize the **1**-P conformer can be precluded by an increasing rotation energy when systematically rotating the different dihedral angles between the carbazole moieties (Figure S57), suggestive of a substantially high configurational stability of **1** with a large racemization energy barrier.

Electronic structures calculated for **1** and **2** using DFT (B3LYP-D3/6-31G*) and TD-DFT (PBE1PBE/6-31G*) are described in Figure 2a and SI. **1** shows a HOMO (–5.28 eV) that is mainly delocalized over the electron-rich carbazole trimers of the figure-of-eight skeleton, while the LUMO (–1.24 eV) is centered on the spirobifluorene linker as a weak electron-acceptor in this structure. In comparison, the HOMO (–4.68 eV)

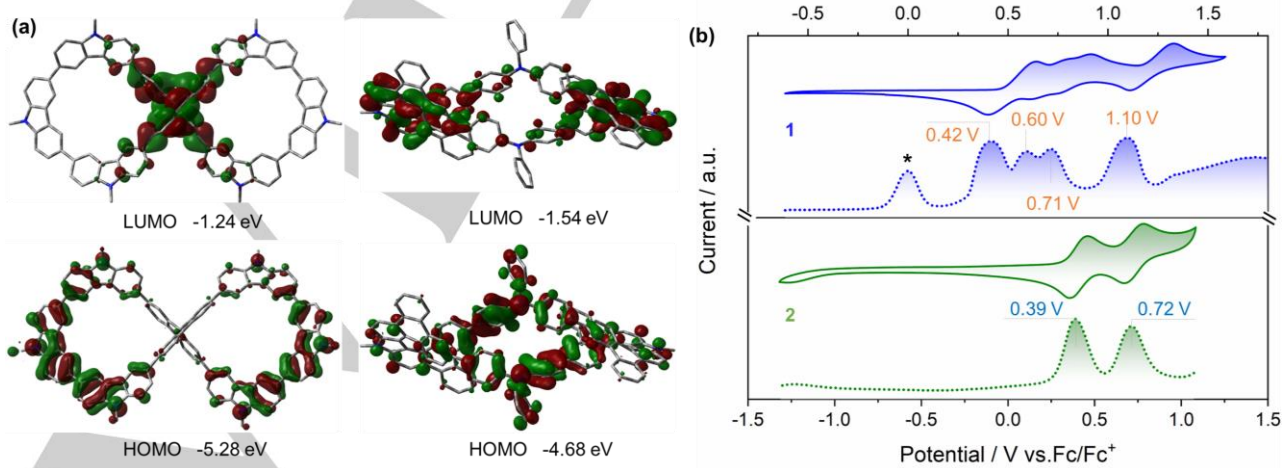

Figure 2. (a) Computed frontier orbital plots of the simplified **1** and **2** (DFT, B3LYP-D3/6-31G*, iso=0.02). (b) Cyclic voltammogram (CV, solid lines) and differential pulse voltammogram (DPV, dashed lines) recorded for the oxidation waves of **1** (blue) and **2** (green) in CH_2Cl_2, *vs* Fc/Fc^+ with *n*-Bu_4NPF_6 (*c* = 0.1 M) as electrolyte, v = 100 mV/s. Fc is indicated by the asterisk.

10.1002/ange.202402800

RESEARCH ARTICLE

Table 1. Summary of the photophysical, computational and electrochemical data of **1** and **2**.

	λ_{abs}[a] (nm)	λ_{em}[a] (nm)	Φ_{FL}[b] (%)	τ_{av}[c] (ns)	E_{gap}[d] (eV)	E_{TDDFT}[e] (eV)	$E_{ox(1)}$[f] (V)	$E_{optical}$[g] (V)
1	245, 310	425	26	4.1	4.04	3.50	0.42	3.08
2	340, 438	480	99	4.0	3.14	2.87	0.39	2.64

[a] Recorded in CH_2Cl_2 (c = 1.0 × 10^{-5} M). [b] Emission quantum yield (Φ_{FL}) in CH_2Cl_2. [c] Emission lifetimes in CH_2Cl_2. [d] Obtained by DFT calculations (B3LYP-D3/6-31G*) and HOMO–LUMO energy gaps: $\Delta E_{DFT} = E_{LUMO} - E_{HOMO}$. [e] Vertical excitation of the lowest energy transition ($S_0 \rightarrow S_1$) calculated by TD-DFT (PBE1PBE, 6-31G*). [f] $E_{ox(1)}$ were determined from the first oxidation peak in DPV scans recorded in 2 mM CH_2Cl_2 under N_2, *vs* Fc/Fc^+ with $[NBu_4]PF_6$ (c = 0.1 M) as the electrolyte, v =100 mV/s. [g] Optical energy gap ($\Delta E_{optical}$) obtained from the onset of lowest energy absorption band in CH_2Cl_2.

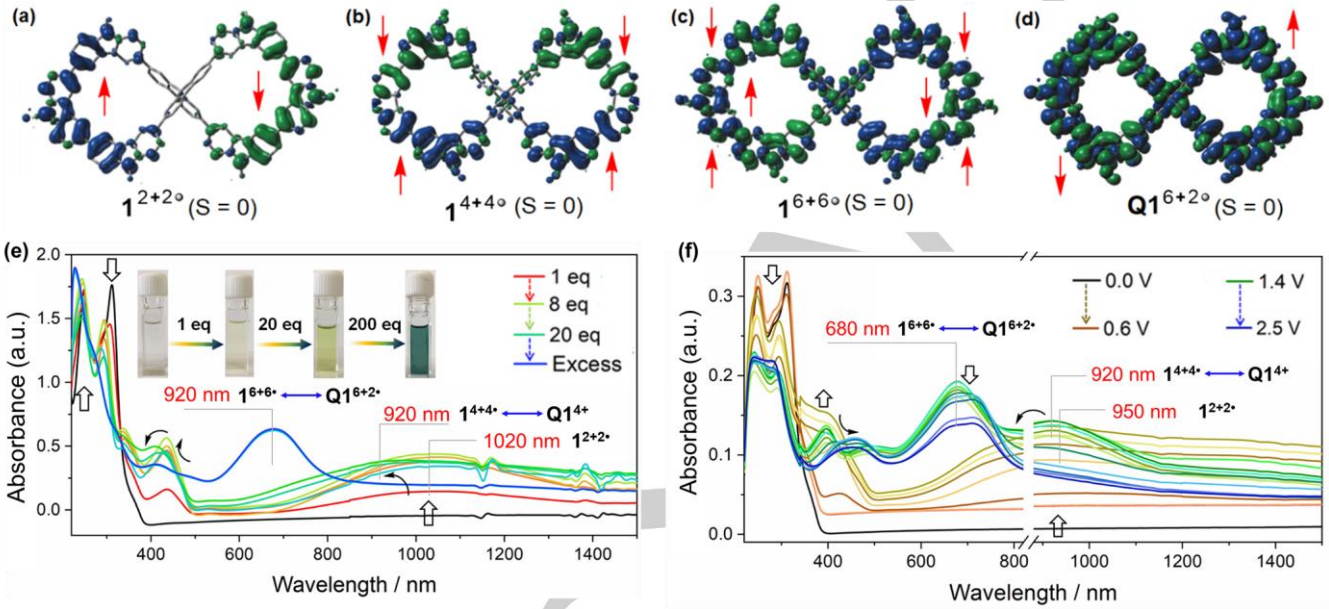

Figure 3. (a,b,c,d) The calculated spin density distribution maps of the lowest-energy oxidized radical cation species ($\mathbf{1}^{2+2\bullet}$, $\mathbf{1}^{4+4\bullet}$, $\mathbf{1}^{6+6\bullet}$ and $\mathbf{Q1}^{6+2\bullet}$) at different oxidization states (DFT/UB3LYP-D3, 6-31G*). (e) Chemical oxidations of **1** (c = 5 × 10^{-5} M, CH_2Cl_2/CH_3CN) with different amounts of $NOSbF_6$ monitored by UV−vis−NIR absorption spectra. Inset: photographs of solutions after the addition of $NOSbF_6$. (f) In situ UV/Vis-NIR spectra monitored by spectroelectrochemical measurements in CH_2Cl_2 upon the oxidation of **1** at increased scan potentials (0–2.5 V).

of **2** is distributed on the stronge donors of triarylamine moieties with a small contribution from the terminal phenyl groups of aza[7]helicenes, but the LUMO (–1.54 eV) is nearly dominated by the aza-[7]helicene moieties. The vertical excitation energy calculated for **2** (E_{TDDFT}: 2.87 eV) is lower than that for **1** (E_{TDDFT}: 3.50 eV) is obviously higher than **1** (-5.28), which is fully consistent with the optical energy gaps (Table 1) and likely indicates a stronger charge-transfer effect in **2**. Cyclic and differential pulse voltammetry (CV and DPV) scans of **1** show likely two reversible two-electron oxidation waves as well as the other two one-electron oxidations in CH_2Cl_2 with the half-wave potentials ($E_{1/2}$) at 0.42, 0.60, 0.71, and 1.10 V vs (Fc/Fc^+) (Figure 2b and SI). Compound **2** displays two reversible oxidation waves at $E_{1/2}$ = 0.39, and 0.72 V, corresponding to the two-step two-electron oxidations of N centers on the triarylamine and aza[7]helicene units, respectively.

Incorporation of multiple sites of main-group electron-donating moieties in macrocycles may enable the consecutive generation of polycationic open-shell chiral cyclophanes with redox-dependent electronic states. To ascertain the stepwise mechanisms associated with this concept, sequentially controlled oxidation experiments were performed for **1** and **2** both chemically and electrochemically. As shown in Figures 3e and S23, the first attempts to oxidize chiral macrocycle **1** in CH_2Cl_2/CH_3CN gave rise to a detectable deep-colored visible change through the chemical oxidation titrations with $NOSbF_6$. As monitored by the UV-vis-NIR spectroscopy, the new absorption band developing after addition of 1.0 equiv $NOSbF_6$ is broader and extends further to a significantly higher wavelength (~1050 nm) as compared with the initial sharp absorption peaks below 400 nm. Upon the addition of increased number of $NOSbF_6$ at room temperature under an inert atmosphere, the main absorption spectra of the resulting reaction systems are gradually blue-shifted to 1020 nm, then 920 nm, and after the full oxidation, a strong absorption profile is observed at 680 nm for a dark green solution. These observations suggest a gradual build-up pathway of the oxidation states from the neutral carbazole-rich macrocycle to a highly charged polycationic cyclophane, which involves formation of a series of open-shell radical cations as shown in Scheme 1.

The above-mentioned oxidation sequences were also well reproduced by the spectroelectrochemical technique under the increased scanning potentials up to 2.5 V, consistent with the chemical-oxidation-induced spectral shifts in the UV-vis-NIR absorption (Figure 3f and S25). We then identified all the possible intermediate cations of this reaction process that experienced with the first oxidations on the opposite carbazole moieties from both sides of the molecule (Figure S38). For each step, the electron spin resonance (ESR) measurements revealed a

10.1002/ange.202402800

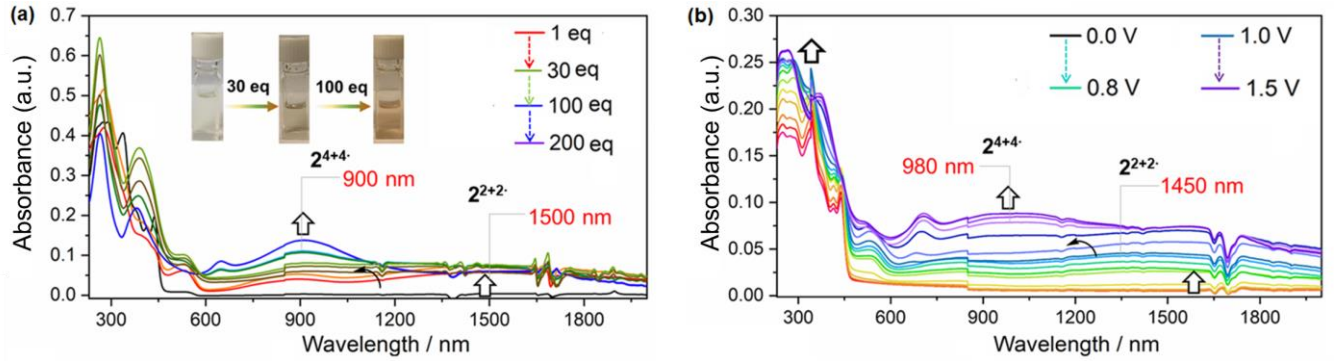

Figure 4. (a) Chemical oxidations of **2** (c = 5 × 10^{-5} M, CH_2Cl_2/CH_3CN) with different amounts of $NOSbF_6$ monitored by UV−vis−NIR absorption spectra. Inset: photographs of solutions after the addition of $NOSbF_6$. (b) In situ UV/Vis-NIR spectra monitored by spectroelectrochemical measurements in CH_2Cl_2 upon the oxidation of **2** at increased scan potentials (0–1.5 V).

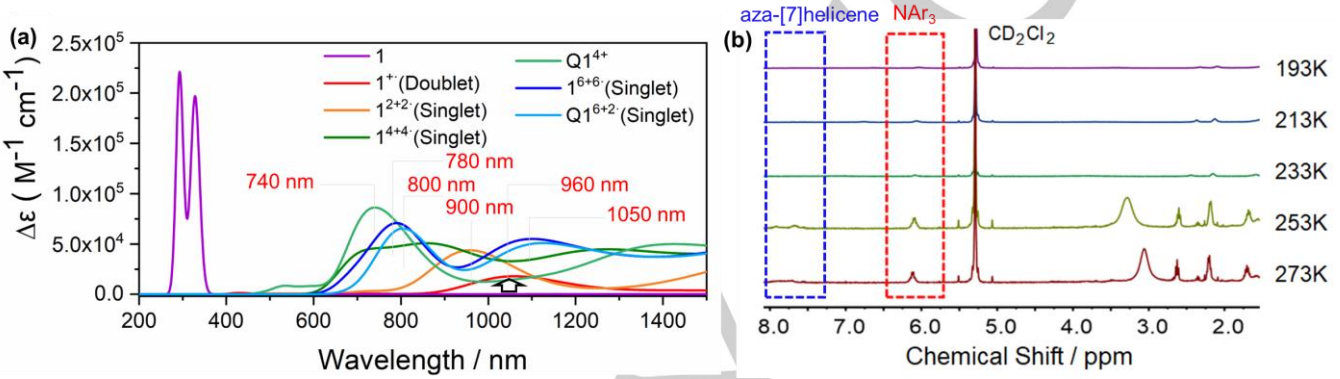

Figure 5. The calculated electronic absorption spectra of (a) **1**, doublet $\mathbf{1}^{\bullet+}$, singlet radical cations ($\mathbf{1}^{2+\bullet}$, $\mathbf{1}^{4+4\bullet}$ and $\mathbf{1}^{6+6\bullet}$) and resonant form ($\mathbf{1}^{4+}$ and $\mathbf{1}^{6+2\bullet}$(singlet)) using TDDFT-PBE1PBE/6-31G* with 40 transition states; (b) partial VT ^{1}H NMR spectra (400 MHz, CD_2Cl_2) of $\mathbf{2}^{2+2\bullet}\mathbf{2SbF_6^-}$ after the addition of 30.0 eq $NOSbF_6$ to **2**.

featureless band of the resulting positively charged cationic species, indicative of an open-shell character due to the loss of electrons from the $N_{carbazole}$ centers (Figure S27). Radical species at higher oxidation states (II, IV and VI) show in principle many possibilities of the spin multiplicity, such as singlet / triplet for $\mathbf{1}^{2+2\bullet}\mathbf{2SbF_6^-}$, singlet / triplet / quintet for $\mathbf{1}^{4+4\bullet}\mathbf{4SbF_6^-}$, $\mathbf{Q1}^{4+}\mathbf{4SbF_6^-}$, singlet / triplet / quintet / septet for $\mathbf{1}^{6+6\bullet}\mathbf{6SbF_6^-}$ and singlet / triplet for $\mathbf{Q1}^{6+2\bullet}\mathbf{6SbF_6^-}$ (Figures S39–S42). Importantly, also energetically, these polycationic radicals were predicted to be all in the singlet ground state, according to the computational results that show the lowest energy levels for positively charged species with a total spin S = 0 (UB3LYP-D3/6-31G*, Table S17, Figures S64–81). Consequently, the identification of such polycations as singlet radicals would be appropriate and reliable. While the tetracation species is likely dominated by $\mathbf{1}^{4+4\bullet}\mathbf{4SbF_6^-}$ where the two radical centers are spaced with a carbazolyl group on each side of the molecule due to charge repulsion (Figure 3c), radical pairing for the adjacent carbazole moieties can also occur, leading to the resonant quinoid structure $\mathbf{Q1}^{4+}\mathbf{4SbF_6^-}$. Similarly, paired radicals are expected to be the case in the formation of higher hexacations $\mathbf{1}^{6+6\bullet}\mathbf{6SbF_6^-}$/$\mathbf{Q1}^{6+2\bullet}\mathbf{6SbF_6^-}$, consistent with the slightly broadened high-energy bands of the hypsochromically shifted absorptions (Figure 3f and Figure 5a).

The computational absorptions modeled for the singlet open-shell species (TDDFT-PBE1PBE/6-31G*) show the same trend as that experimentally observed from the UV-vis-NIR profiles (Figure 5a and others in SI). The spin density maps (UB3LYP-D3, 6-31G*) are not localized to small segments of the oxidized carbazole moieties but are truly delocalized along the macrocyclic skeletons (Figure 3a–3d), contributing also to persistence of the chiral radical cations with increasing number of charges (Figure S50 and S51). To better understand the spin-spin interactions, we selected the species that is predicted to be dominated by diradical dication $\mathbf{1}^{2+2\bullet}\mathbf{2SbF_6^-}$ as a representative example, corresponding to the additiona of 20 equiv of $NOSbF_6$.[23] The structureless one-line ESR spectra showed a gradual decrease of the signal intensity as temperature decreased from 150 down to 100 K, indicating a singlet ground state in $\mathbf{1}^{2+2\bullet}\mathbf{2SbF_6^-}$ (Figure 6a). Fitting of the variable-temperature (VT-ESR) data with the Bleaney-Bowers equation furnished an experimental singlet–triplet energy gap ($\Delta E_{S\text{-}T}$ = –1.29 kcal mol^{-1}) (Figure 6b), in accord with the theoretical computation ($\Delta E_{S\text{-}T}$ = –0.66 kcal mol^{-1}, UB3LYP/6-31G*) with a diradical character index y_0 = 0.85 (see the SI).

Similar characterizations were performed for another chiral macrocycle **2** in the chemically and electrochemically oxidative environments. As shown in Figure 4a, the use of less than 30 equivalents of $NOSbF_6$ leads to the two new absorption bands at 1500 and 900 nm in the long-wavelength region of UV-vis-NIR spectra. This can be attributed to oxidations of the triphenylamine donor sites by comparing the absorption profiles to those via spectroelectrochemical measurements at low oxidation potentials (Figure 4b). The formed dications under this condition were used for the ESR and ^{1}H NMR spectroscopic characterization. A significant line broadening assigned to the triarylamine (NAr_3) and aza[7]helicene moieties in ^{1}H NMR spectrum at low temperature suggests the open-shell diradical character. Furthermore, variable-temperature NMR (VT-NMR) spectroscopy studies show that these broadened signals at 193 K become increasingly resolved sharp ones as the sample is warmed back up to 273 K (Figure 5b and S37), indicative of the presence of ground-state

10.1002/ange.202402800

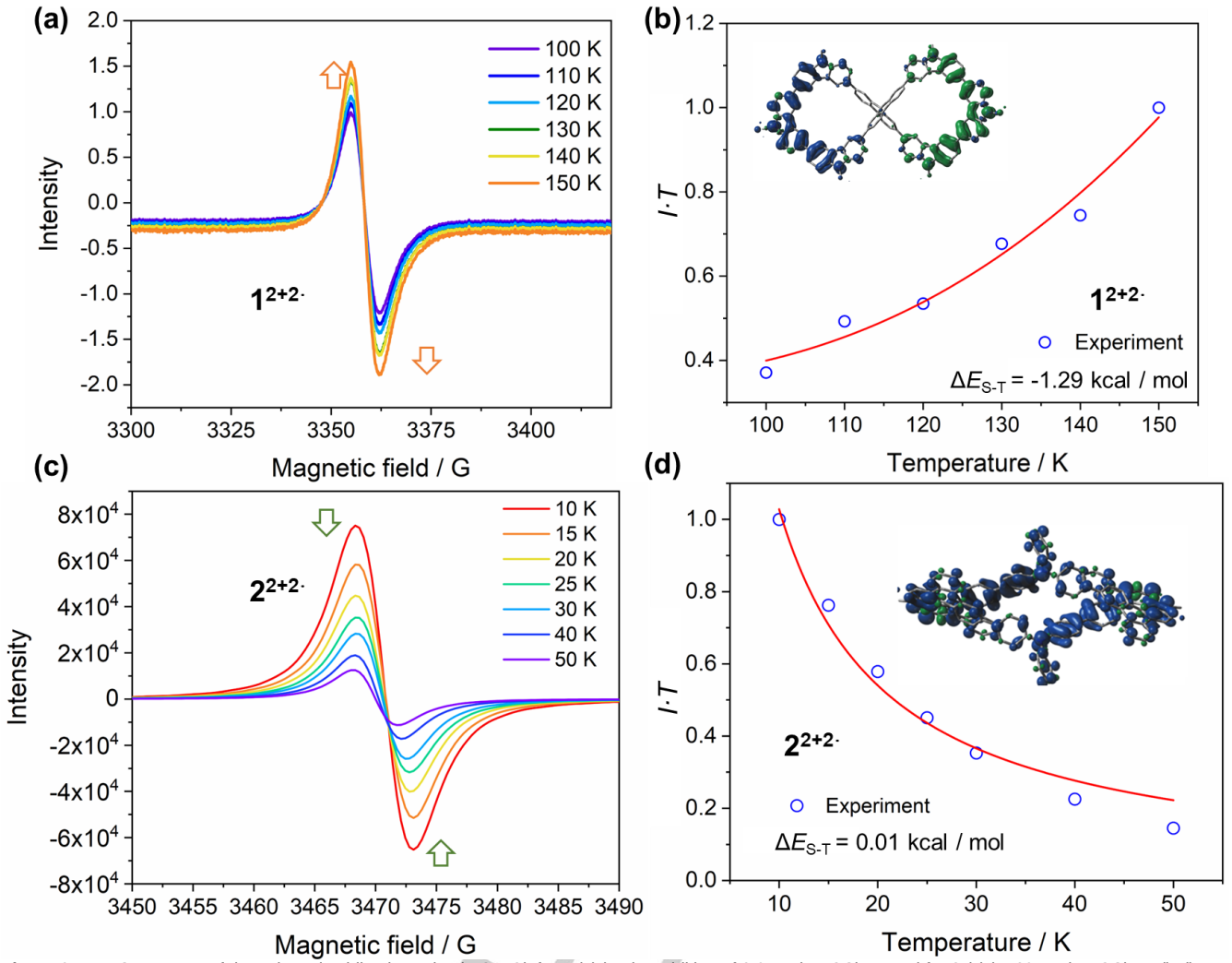

Figure 6. VT-ESR spectra of the selected oxidized species in CH_2Cl_2 for **1** (a) by the addition of 8.0 equiv $NOSbF_6$, and for **2** (c) by 20 equiv $NOSbF_6$. (b,d) *IT*–*T* plots of the diradical cation species used for the VT-ESR studies. The red lines are the Bleaney–Bowers fit of the data. Inset: the calculated spin density distribution map (DFT-UB3LYP-D3, 6-31G*).

triplet diradical $\mathbf{2}^{2+2\bullet}\mathbf{2SbF_6}^-$.

The structureless ESR spectrum with *g*-value of 2.003 can further support a paramagnetic nature of the open-shell species $\mathbf{2}^{2+2\bullet}\mathbf{2SbF_6}^-$, and its ESR intensity gradually increases with decreasing temperature within 10–50 K (Figure 6c). Fitting of the VT-ESR data in the Bleaney-Bowers equation gave an experimental $\Delta E_{S\text{-}T}$ = 0.01 kcal mol^{-1} (Figure 6d), a positive singlet–triplet energy gap, likely reflective of the triplet ground state diradicals. In general, such a small energy gap may indicate a degenerate singlet / triplet state of $\mathbf{2}^{2+2\bullet}\mathbf{2SbF_6}^-$, which can be rationalized by the computed value $\Delta E_{S\text{-}T}$ of –0.15 kcal mol^{-1} (UB3LYP-D3/6-31G*) with a very low-lying triplet state and a diradical character index y_0 = 0.64 (see the SI). Further titrations of diradical dication $\mathbf{2}^{2+2\bullet}\mathbf{2SbF_6}^-$ with an excess of $NOSbF_6$ only resulted in an increased absorption band at ~900 nm, caused by the follow-up oxidations of N centers in aza[7]helicene moieties (Figure 4). In comparison to $\mathbf{2}^{2+2\bullet}\mathbf{2SbF_6}^-$, the resulting tetraradical tetracation $\mathbf{2}^{4+4\bullet}\mathbf{4SbF_6}^-$ remained the fine-structured ESR but with an enhanced magnetic response intensity (Figure S28). It is also noteworthy that the spin-delocalization onto the π-skeletal chiral cyclophanes is predicted for both $\mathbf{2}^{2+2\bullet}\mathbf{2SbF_6}^-$ and $\mathbf{2}^{4+4\bullet}\mathbf{4SbF_6}^-$ at different oxidation states (Figure S44 and S45). The calculated absorption data are in agreement with those curves recorded in the UV-vis-NIR spectra (Figure S91).

These open-shell polycationic species display the high stability in CH_2Cl_2 as no significant decomposition was detected in the UV-vis-NIR absorption spectra after the storage within 7 days at room temperature under N_2 (Figure S33–S35). The unique low-energy absorption extending to the NIR domain presumably enables the chiral radical cations (Figure S50–S52) to be employed for future applications in chiroptoelectronic materials, spin filters and phototherapy.[24] The obtained open-shell radical cyclophanes could also be readily switched to the initial closed-shell structure, which was evidenced by the fact that the resolved ^{1}H NMR signals were recovered from the highly broadened resonances upon the addition of triethylamine to the oxidized cation intermediates (Figure S36).

UV-vis absorption and emission spectra were examined for neutral states of **1** and **2** in CH_2Cl_2. As shown in Figure 7a, the absorption profiles are mainly distributed within the short wavelength region. For **1**, the main absorption bands at ~245 and 310 nm correspond to the π-π* transitions, and a red-shifted

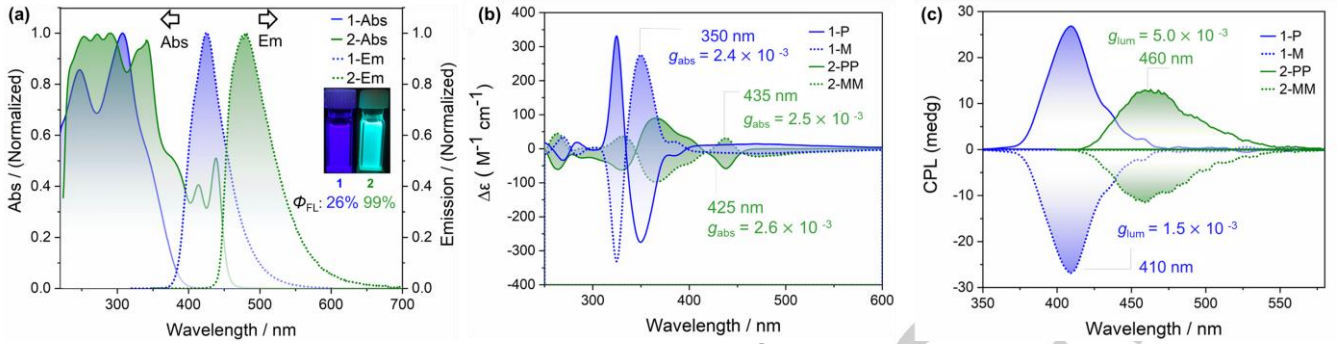

Figure 7. (a) UV-vis absorption and emission spectra ($\lambda_{ex} = \lambda_{abs(max)}$) in CH_2Cl_2 (c = 1.0 × 10^{-5} M). Inset: photographs of emission in CH_2Cl_2 under 365 nm UV light; (b) circular dichroism spectra and (c) circularly polarized luminescence spectra of **1** and **2** (c =1.0 × 10^{-5} M) in CH_2Cl_2 at 298 K.

shoulder band was also observed at round 350 nm, which can be ascribed to a weak intramolecular charge transfer (ICT) from the electron-rich carbazolyl units to the central spirobifluorene moiety. However, the absorption peaks for macrocycle **2** are broader and extend to significantly higher wavelengths (340 and 438 nm) than those for **1** as a result of the π-conjugation extension of aza[7]helicenes as compared with the bare carbazole moieties. Both chiral macrocycles are intense fluorescent (**1**: λ_{em} = 425 nm; **2**: λ_{em} = 480 nm), and **2** shows a nearly quantitative emission quantum efficiency (Φ_{FL} = 0.99) in CH_2Cl_2 (Table 1).

Chiroptical properties of **1** and **2** in the ground states were characterized by circular dichroism (CD) (Figures 7b and S48). The enantiomers of each macrocycle show mirror images with opposite Cotton effects in CD spectra, and the anisotropy factors ($|g_{abs}|$, defined as $\Delta\varepsilon/\varepsilon$) were quantified to be 2.40 × 10^{-3} for **1** at 350 nm and 2.50 × 10^{-3} for **2** at 435 nm. To further identify the main peaks in CD spectra, TD-DFT calculations were performed at the PBE1PBE/6-31G* level (Table S9 and S10). The lowest-energy absorption peak can be attributed to the $S_0 \rightarrow S_3$ and $S_0 \rightarrow S_4$ transitions for **1**, whereas the corresponding absorption band for **2** is assigned to the $S_0 \rightarrow S_1$ transition (Figure S48). The absorption dissymmetry factors were also estimated by the equation $g_{abs} = 4 \cos\theta|m||\mu|/(|m|^2 + |\mu|^2)$, wherein μ, m, and θ represent the electric and magnetic transition dipole moments as well as the angle between μ and m, respectively, leading to the theoretical values of 3.3 × 10^{-2} for **1** and 1.4 × 10^{-2} for **2** corresponding to their lowest-energy absorption peak ($S_0 \rightarrow S_1$, TDDFT-PBE1PBE/6-31G*, Figure S55 and S56). The absolute configurations have been simulated by the calculated electronic circular dichroism (ECD) spectra (TDDFT-PBE1PBE/6-31G*), with the first fraction in HPLC profiles assigned to the **1**-P / **2**-PP and the second to the **1**-M / **2**-MM stereomers (Figures S55, S56).

We also recorded the chiroptical properties of **1** and **2** in the excited states by the mirror-imaged CPL spectra in CH_2Cl_2. The luminescence dissymmetry factors (g_{lum}) were measured to be 1.50 × 10^{-3} at 410 nm for **1**-P and 5.00 × 10^{-3} at 460 nm for **2**-PP (Figure 7c). There is only a negligible change in the two sets of values (g_{lum} and g_{abs}), suggesting that the ground state and emitting excited-state molecules show a similar geometry for both figure-of-eight chiral macrocycles. Using the well-established equation of CPL brightness ($B_{CPL} = \varepsilon \times \Phi_{FL} \times g_{lum}/2$), the overall chiroptical performance of CPL-active materials can be quantified by the three optical parameters.[25] The B_{CPL} values were calculated to be 42.7 and 100.2 M^{-1} cm^{-1} for **1** and **2**, respectively. The B_{CPL} for the figure-of-eight macrocycle **1** is among the highest ones reported for organic π-conjugated chiral macrocycles,[22] which could find promising applications in CP-OLED related areas.

Conclusion

We have described the synthetic approaches to achieve π-conjugated new macrocycles (**1** and **2**) with a molecular chirality due to the unique (*quasi*) figure-of-eight conformations using the 2,2',7,7'-spirobifluorenyl fragment and aza[7]helicene moieties as the key linkage components, respectively. Both macrocycles are strongly luminescent with an approximately quantitative emission quantum efficiency for **2** in CH_2Cl_2 and with a high CPL brightness (B_{CPL}= 100.2 $M^{-1}cm^{-1}$). Most interestingly, these structures are electron-rich in nature, and they represent the rarely obtained chiral macrocycles where the structures in neutral states can be transformed into the highly charged ones under mild conditions. The chemically and electrochemically controlled oxidations of **1** and **2** resulted in the sequential formation of polycationic chiral cyclophanes with multispin open-shell characters, which are commonly inaccessible in the all-carbon-based analogues. The redox-dependent electronic states were evidenced magnetically and spectroscopically. This early work showcases a distinct pathway to fully charged high oxidation-state chiral species with potential applications in organic spintronics and superconductors as well as assembled superstructures. Synthesis of highly charged new chiral main-group macrocycles with ground state high-spin diradicals and polyradicals is underway in our laboratory.

Experimental Section

Experimental procedures, analytic data (^{1}H, ^{13}C and HRMS) for all products and intermediates, photophysical and electrochemical data, calculations in the ground state and excited-state computations.

Acknowledgements

This work was supported by the National Natural Science Foundation of China (Nos. 22271013 and 21772012) and also by the Beijing Natural Science Foundation (No. 2232024). We are thankful to Prof. Suning Wang at Queen's University for helpful discussions over years. We thank the Analysis & Testing Centre at Beijing Institute of Technology for advanced facilities.

Keywords: Open-Shell Cyclophanes • Luminescent Chiral Macrocycle • Figure-of-Eight • Polycations • Radical Chirality

[1] a) A. Samanta,Z. Liu, S.K. Mohan Nalluri,Y. Zhang,G. C. Schatz and J. F. Stoddart, *J. Am. Chem. Soc.* **2016**, *138*, 14469–14480; b) A. Dey, S. Chand, L. O. Alimi, M. Ghosh, L. Cavallo and N. M. Khashab, *J. Am. Chem. Soc.* **2020**, *142*, 15823–15829; c) W.Shang, X. F. Zhu, Y. Jiang, J. Cui, K. Liu, T. Li, M. Liu, *Angew. Chem.Int. Ed.* **2022**, *61*, e202210604; *Angew. Chem.* **2022**, *134*, e202210604; d) Y. Fan, J. He, L. Liu, G. Liu, S. Guo, Z. Lian, X. Li, W. Guo, X. Chen, Y. Wang, H. Jiang, *Angew. Chem. Int. Ed.* **2023**, *62*, e202304623; *Angew. Chem.* **2023,** *135*, e202304623; e) López, R.; Palomo, C., *Angew. Chem. Int. Ed.,* **2022,** *61*, e202113504; *Angew. Chem.* **2022**, *134*, e202113504.

[2] a) H. Jędrzejewska, A. Szumna, *Chem. Rev.* **2017**,*117*, 4863–4899; b) L. J. Chen, H. B. Yang, M. Shionoya, *Chem. Soc. Rev*. **2017**, *46*, 2555–2576; c) M. Kwit, J. Grajewski, P. Skowronek, M. Zgorzelak, J. Gawronski, *Chem. Rev.* **2019**, *19*, 213–237; d) N. E. Borisova,M. D. Reshetova, Y. A. Ustynyuk, *Chem. Rev.* **2007**, *107*, 46–79; e) Y. Wang, H. Wu, J. F. Stoddart, *Acc. Chem. Res.* **2021**, *54*, 2027–2039; f) M. Hasegawa, Y. Nojima, Y. Mazaki, *Chem Photo Chem.* **2021**, *5*, 1042–1058.

[3] a) S.Hitosugi, Wa. Nakanishi, T. Yamasaki, H. Isobe, *Nat. Commun.,* **2011**, *2*, 492; b) S. Hitosugi, T. Yamasaki and H. Isobe, *J. Am. Chem. Soc.*, **2012**, *134*, 12442–12445; c) T. Matsuno, S. Kamata, S. Hitosugia, and H. Isobe, *Chem. Sci.*, **2013**, *4*, 3179–3183; d) K. Kogashi, T. Matsuno, S. Sato, H. Isobe, *Angew. Chem. Int. Ed.*, **2019**, *58*, 7385–7389; *Angew. Chem.* **2019**, *131*, 7463–7467; e) J. Wang, G. Zhuang, M. Chen, D. Lu, Z. Li, Q. Huang, H. Jia, S. Cui, X. Shao, S. Yang and P. Du, *Angew. Chem. Int. Ed.,* **2020**, *59*, 1619–1626; *Angew. Chem.* **2020**, *132*, 1636–1643; f) J. Wang, H. Shi, S. Wang, X. Zhang, P. Fang, Y. Zhou, G. L. Zhuang, X. Shao and P. Du, *Chem. Eur. J.,* **2022**, *28*, e202103828; g) J. He, M. Yu, M. Pang, Y. Fan, Z. Lian, Y. Wang, W. Wang, Y. Liu and H. Jiang, *Chem. Eur. J.*, **2022**, *28*, e202103832; h) W. Xu, Y. Nagata, N. Kumagai, *J. Am. Chem. Soc.,* **2023,** *145*, 2609–2618.

[4] a) K. Senthilkumar, M. Kondratowicz, T. Lis, P. J. Chmielewski, J. Cybińska, J. L. Zafra, J. Casado, T. Vives, J. Crassous, L. Favereau, and M. Stępień, *J. Am. Chem. Soc.*, **2019**, *141*, 7421–7427; b) L. H. Wang, J. Nogami, Y. Nagashima, and K. Tanaka, *Org. Lett.,* **2023**, *25*, 4225–4230; c) A. Robert, G. Naulet, H. Bock, N. Vanthuyne, M. Jean, Michel Giorgi, Y. Carissan, C. Aroulanda, A. Scalabre, E. Pouget, F. Durola and Y. Coquerel, *Chem. Eur. J.*, **2019**, *25*, 14364–14369; d) G. R. Kiel, K. L. Bay, A. E. Samkian, N. J. Schuster, J. B. Lin, R. C. Handford, C. Nuckolls, K. N. Houk, and T. D. Tilley, *J. Am. Chem. Soc.*, **2020**, *142*, 11084–11091; e) Y. Li, A. Yagi, and K. Itami, *J. Am. Chem. Soc.*, **2020**, *142*, 3246–3253; f) L. H. Wang, N. Hayase, H. Sugiyama, J. Nogami, H. Uekusa, and K. Tanaka, *Angew. Chem. Int. Ed.*, **2020**, *59*, 17951–17957; *Angew. Chem.* **2020**, *132*, 18107–18113; g) W. Xu, X. D. Yang, X. B. Fan, X. Wang, C. H. Tung, L. Z. Wu and H. Cong, *Angew. Chem. Int. Ed.*, **2019**, *58*, 3943-3947; *Angew. Chem.* **2019**, *131*, 3983–3987; h) X. Zhang, H. Liu, G. Zhuang, S. Yang and P. Du, *Nat Commun.*, **2022**, *13*, 3943–3947; i) T. Terabayashi, E. Kayahara, Y. C. Zhang, Y. Mizuhata, N. Tokitoh, T. Nishinaga, T. Kato, Shigeru. Yamago, *Angew. Chem. Int. Ed.,* **2023**, *62*, e2022149; *Angew. Chem.* **2023**, *135*, e202214960; j) G. R. Schaller, F. Topić, K. Rissanen, Y. Okamoto, J. Shen, R. Herges, *Nat. Chem.,* **2014**, *6*, 608; k) Q. F. Zhou, X. D. Hou, J. Y. Wang, Y. Ni, W. Fan, Z. T. Li, X. Wei, K. Li, W. Yuan, Z. F. Xu, M. Z. Zhu, Y. L. Zhao, Z. Sun, J. S. Wu, *Angew. Chem. Int. Ed.,* **2023**, *62*, e202302266; *Angew. Chem.* **2023**, *135*, e202302266; l) M. C. O'Sullivan, J. K. Sprafke, D. V. Kondratuk, C. Rinfray, T. D. W. Claridge, A. Saywell, M. O. Blunt, J. N. O'Shea, P. H. Beton, M. Malfois, H. L. Anderson. *Nature*, **2011**, *469*, 72-75; m) M. Pawlicki, M. Morisue, N. Davis, D. McLean, J. E. Haley, E. Beuerman, M. Drobijev, A. Rebane, A. L. Thompson, S. I. Pascu, G. Accorsi, N. Armaroli, H. L. Anderson. *Chem. Sci.*, **2012**, *3*, 1541-1547; n) D. V. Kondratuk, J. K. Sprafke, M. C. O'Sullivan, L. M. A. Perdigão, A. Saywell, M. Malfois, J. N. O'Shea, P. H. Beton, A. L. Thompson, H. L. Anderson. *Chem. - Eur. J.*, **2014**, *20*, 12826; o) S. Liu, D. V. Kondratuk, S. A. L. Rousseaux, G. Gil-Ramírez, M. C. O'Sullivan, J. Cremers, T. D. W. Claridge, H. L. Anderson. *Angew. Chem. Int. Ed.*, **2015**, *54*, 5355-5359; *Angew. Chem.* **2015**, *127*, 5445-5449; p) G. Gil-Ramírez, A. Shah, H. El Mkami, K. Porfyrakis, G. A. D. Briggs, J. J. L. Morton, H. L. Anderson, J. E. Lovett. *J. Am. Chem. Soc.*, **2018**, *140*, 7420-7424.

[5] a) J. Malinčík, S. Gaikwad, J. P. M. Fuentes, M. A. Boillat, A. Prescimone, D. Häussinger, A. G. Campaña and T. Šolomek, *Angew. Chem. Int. Ed.*, **2022**, *61*, e202208591; *Angew. Chem.* **2022**, *134*, e202208591; b) G. Naulet, L. Sturm, A. Robert, P. Dechambenoit, F. Röhricht, R. Herges, H. Bocka and F. Durola, *Chem. Sci.*, **2018**, *9*, 8930–8936; c) X. Jiang, J. D. Laffoon, D. Chen, S. Perez-Estrada, A. S. Danis, J. Rodríguez-Lopez, M. A. Garcia-Garibay, J. Zhu and J. S. Moore, *J. Am. Chem. Soc.*, **2020**, *142*, 6493–6498; d) Y. Segawa, T. Watanabe, K. Yamanoue, M. Kuwayama, K. Watanabe, J. Pirillo, Y. Hijikata and K. Itami, *Nat. Syn.*, **2022**, *1*, 535–541; e) J. He, M. H. Yu, Z. Lian, Y. Q. Fan, S. Z. Guo, X. N. Li, Y. Wang, W. G. Wang, Z. Y. Cheng and H. Jiang, *Chem. Sci.,* **2023**, *14*, 4426–4433.

[6] a) A. Yagi, Ya. Segawa, K. Itami, *Chem.*, **2019**, *5*, 746–748; b) K. Y. Cheung, S. J. Gui, C. F. Deng, H. F. Liang, Z. M. Xia, Z. F. Liu, L. F. Chi, Q. Miao, *Chem.*, **2019**, *5*, 838–847; c) S. Nishigaki, Y. Shibata, A. Nakajima, H. Okajima, Y. Masumoto, T. Osawa, A. Muranaka, H. Sugiyama, A. Horikawa, H. Uekusa, H. Koshino, M. Uchiyama, A. Sakamoto and K. Tanaka, *J. Am. Chem. Soc.*, **2019**, *141*, 14955–14960; d) J. Nogami, Y. Tanaka, H. Sugiyama, H. Uekusa, A. Muranaka, M. Uchiyama and Tanaka, *J. Am. Chem. Soc.*, **2020**, *142*, 9834–9842; e) J. Nogami, Y. Nagashima, K. Miyamoto, A. Muranaka, M. Uchiyamabc and K. Tanaka, *Chem. Sci.*, **2021**, *12*, 7858–7865; f) W. Fan, T. Matsuno, Y. Han, X. Wang, Q. Zhou, H. Isobe and J. Wu, *J. Am. Chem. Soc.*, **2021**, *143*, 15924–15929; g) M. Krzeszewski, H. Ito and K. Itami, *J. Am. Chem. Soc.*, **2022**, *144*, 862–871; h) J. Nogami, Y. Nagashima, H. Sugiyama, K. Miyamoto, Y. Tanaka, H. Uekusa, A. Muranaka, M. Uchiyama and K. Tanaka, *Angew. Chem. Int. Ed.*, **2022**, *61*, e202200800; *Angew. Chem.* **2022**, *134*, e202200800; i) X. S. Du, X. N. Han, Y. Han and C. F. Chen, *Chem. Commun.*, **2023**, *59*, 227–230; j) Q. Zhou, X. Hou, J. Wang, Y. Ni, W. Fan, Z. Li, X. Wei, K. Li, W. Yuan, Z. Xu, M. Zhu, Y.i Zhao, Z. Sun, J. Wu, *Angew. Chem. Int. Ed.*, **2023**, *62*, e202302266; *Angew. Chem.* **2023**, *135*, e202302266; k) Z. Y. Jiang, H. Xiao, S. Tong, T. H. Shi, J. P. Zhu, M. X. Wang, *Angew. Chem. Int. Ed.,* **2023**, *62*, e2023017; *Angew. Chem.* **2023**, *135*, e2023017.

[7] a) Y. Ohishi, M. Murase, H. Abe and Masahiko Inouye, *Org. Lett.*, **2019**, *21*, 6202–6207; b) K. Sato, M. Hasegawa, Y. Nojima, N. Hara, T. Nishiuchi, Y. Imai and Y. Mazaki, *Chem. Eur. J.*, **2021**, *27*, 1323–1329; c) P. Fang, M. Chen, X. Zhang and P. Du, *Chem. Commun*., **2022**, *58*, 8278–8281; d) Q. Huang, J. Zhang, H. Chen, X. Kong, P. Xu and P. Du, *Org. Chem. Front.,* **2023**, *10*, 911–915; e) K. J. Weiland, T. Brandl, K. Atz, A. Prescimone, D. Haussinger, T. Sŏlomek and M. Mayor, *J. Am. Chem. Soc.*, **2019**, *141*, 2104–2110; f) K. Zhu, K. Kamochi, T. Kodama, M. Tobisu and T. Amaya, *Chem. Sci.*, **2020**, *11,* 9604–9610; g) Y. Xu, F. Steudel, M. Y. Leung, B. Xia, M. Delius and V. W. W. Yam, *Angew. Chem. Int. Ed.,* **2023**, *62*, e202302978; *Angew. Chem.* **2023**, *135*, e202302978; h) J. Malinčík, S. Gaikwad, J. P. Mora-Fuentes, M. A. Boillat, A. Prescimone, D. Häussinger, A. G. Campaña, and T. Šolomek, *Angew. Chem. Int. Ed.,* **2022**, *61*, e2022085; *Angew. Chem.* **2022**, 134, e202208591.

[8] a) S. Wu, M. Li, H. Phan, D. Wang, T. S. Herng, J. Ding, Z. Lu, J. Wu, *Angew. Chem. Int. Ed.,* **2018**, *57*, 8007–8011; *Angew. Chem.* **2018**, *130*, 8139–8143; b) I. Ratera,J. Veciana, *Chem. Soc. Rev.***2012**, *41*, 303–349; c) J. Mahmood, J. B. Baek, *Chem*, **2019**, *5*, 1012–1014; d) Q. Jiang, J. Zhang, Z. Mao, Y. Yao, D. Zhao, Y. Jia, D. Hu, Y. Ma, *Adv. Mater.* **2022**, *34*, 2108103; e) B. T. Matthias, R. M. Bozorth, J. H. Van Vleck, *Phys. Rev. Lett.* **1961**, *7*, 160.

[9] a) A. Mauger, C. Godart, *Phys. Rep.***1986**, *141*, 51–176; b) J. K. Furdyna, *J. Appl. Phys.***1988**, *64*, R29–R64; c) H. Ohno, *Science,* **1998**, *281*, 951–956; d) K. Sato, L. Bergqvist, J. Kudrnovský, P. H. Dederichs, O. Eriksson, I. Turek, B. Sanyal, G. Bouzerar, H. Katayama-Yoshida, V. A. Dinh, T. Fukushima, H. Kizaki, R. Zeller, *Rev. Mod. Phys.* **2010**, *82*, 1633; e) T. Dietl, H. Ohno, *Rev. Mod. Phys.* **2014**, *86*, 187; f) K. Ando, *Science,* **2006**, *312*, 1883-1885; g) N. Samarth, *Nat. Mater.* **2010**, *9*, 955–956; h) S. Chambers, *Nat. Mater.* **2010**, *9*, 956–957; i) J. S. Miller, *Adv. Mater.***1994**, *6*, 322; j) R. M. White, *Science*,**1985**, *229*, 11-15; k) J. S. Miller, *Mater. Today*, **2014**, *17*, 224–235.

[10] a) J. Thiele, H. Balhorn, *Chem. Ges.***1904**, *37*, 1463−1470; b) A. E. Tschitschibabin, *Chem. Ges.***1907**, *40*, 1810−1819; c) E. MÜller, H. Pfanz, *Chem. Ges. B,* **1941**, *74*, 1051−1074; d) L. K. Montgomery, J. C. Huffman, E. A. Jurczak, M. P. Grendze, *J. Am. Chem. Soc.***1986**, *108*, 6004−6011; e) J. Wang, X. Xu, H. Phan, T. S. Herng, T. Y. Gopalakrishna, G. Li, J. Ding, J. Wu, *Angew. Chem. Int. Ed.,* **2017**, *56*, 14154–14158; *Angew. Chem.* **2017**, *129*, 14342–14346; f) G. Tan, X. Wang, *Acc. Chem. Res.* **2017**, *50*, 8, 1997–2006; g) Z. Sun, K. Huang, J. Wu, *J. Am. Chem. Soc.* **2011**, *133*, 31, 11896–11899; h) Z. T. Feng, S. X. Tang, Y. T. Su, X. P. Wang, *Chem. Soc. Rev.* **2022**, *51*, 5930–5973.

[11] a) K. Li, Z. Xu, J. Xu, T. Weng, X. Chen, S. Sato, J. Wu, Z. Sun, *J. Am. Chem. Soc.* **2021**, *143*, 20419–20430; b) W. Zeng, J. Wu, *Mater. Chem. Front.,* **2019**, *3*, 2668–2672; c) C. Liu, G. Li, H. Phan, Y. Zou, X. Lu, J. Wu, *Org. Lett.* **2021**, *23*, 4860–4863; d) P. Yadav, S. Das, H. Phan, T. S. Herng , J. Ding, J. Wu, *Org. Lett.* **2016**, *18*, 2886–2889; e) Z. Lim, B. Zheng, K. Huang, Y. Liu, J. Wu, *Chem. Eur. J.* **2015**, *21*, 18724–18729; f) T. Nishiuchi, S. Aibara, H. Sato and T. Kubo, *J. Am. Chem. Soc.* **2022**, *144*, 7479–7488; g) J. Guo, Z. Li, X. Tian, T. Zhang, Y. Wang, C. Dou, *Angew. Chem. Int. Ed.*, **2023**, *62*, e202217470; *Angew. Chem.* **2023**, *135*, e202217470; h) Y. Su, X. Wang, Y. Li, Y. Song, Y. Sui, X. Wang, *Angew. Chem. Int. Ed.*, **2014**, *54*, 1634–1637; *Angew. Chem.* **2014**, *127*, 1654–1657.

[12] a) G. Liu, L. Gao, Y. Han, Y. Xiao, B. Du, J. Gong, J. Hu, F. Zhang, H. Meng, X. Li, X. Shi, Z. Sun, J. Wang, G. Dai, C. Chi, Q. Wang, *Angew. Chem. Int. Ed.*, **2023**, *62*, e202301348; *Angew. Chem.* **2023**, *135*, e202301348; b) G. Xie, N. M. Bojanowski, V. Brosius, T. Wiesner, F. Rominger, J. Freudenberg, U. H. F. Bunz, *Chem. Eur. J.* **2021**, *27*, 1976 –1980; c) G. Xie, V. Brosius, J. Han, F. Rominger, A. Dreuw, J. Freudenberg, U. H. F. Bunz, *Chem. Eur. J.* **2020**, *26*, 160–164; d) G. M. Labrador, C.Besnard, T. Bürgi, A. I. Poblador-Bahamonde, J. Bosson, J. Lacour, *Chem. Sci.*, **2019**, *10*, 7059–7067; e) F. Lopez-Garcia, S. Dong, Y. Han, J. J. C. Lee, P. W. Ng, C. Chi, *Org. Lett.* **2021**, *23*, 6382–6386; f) Y. Chen, H. Kueh, T. Y. Gopalakrishna, S. Dong, Y. Han, C. Chi, *Org. Lett.* **2019**, *21*, 3127–3130; g) X. Shi, W. Kueh, B. Zheng, K. Huang, C. Chi, *Angew. Chem. Int. Ed.*, **2015**, *54*, 14412–14416; *Angew. Chem.* **2015**, *127*, 14620–14624; h) D. Chang, J. Zhu, Y. Sun, K. Chi, Y. Qiao, T. Wang, Y. Zhao, Y. Liu, X. Lu, *Chem. Sci.,* **2023**,*14*, 6087–6094; i) S. Qiu, Y. Zhao, L. Zhang, Y. Ni, Y. Wu, H. Cong, D. Qu, W. Jiang, J. Wu, H. Tian and Z. Wang, *CCS Chem.* **2023**, *5,* 1763–1772; j) S. Das, T. S. Herng, J. L. Zafra, P. M. Burrezo, M. Kitano, M. Ishida, T.Y. Gopalakrishna, P. Hu, A. Osuka, J. Casado, J. Ding, D. Casanova and J. Wu, *J. Am. Chem. Soc.* **2016**, *138*, 7782−7790.

[13] a) H. Zhang, M. Pink, Y. Wang, S. Rajca, A. Rajca, *J. Am. Chem. Soc.* **2022**, *144*, 19576–19591; b) C. Shu, H. Zhang, A. Olankitwanit, S. Rajca, A. Rajca, *J. Am. Chem. Soc.* **2019**, *141*, 17287–17294; c) A. Rajca, C. Shu, H. Zhang, S. Zhang, H. Wang, S. Rajca, *Photochemistry and Photobiology,* **2021**, *97*, 1376–1390; d) M. Miyasaka, M. Pink, S. Rajca, A.Rajca; *Angew. Chem. Int. Ed.,* **2009**, *48*, 5954–5957; *Angew. Chem.* **2009**, *121*, 6068–6071; e) A. Rajca, A. Olankitwanit, Y. Wang, P. J. Boratyński, M. Pink, S. Rajca, *J. Am. Chem. Soc.* **2013**, *135*, 18205–18215; f) M. Abe, *Chem. Rev.* **2013**, *113*, 7011–7088; g) Q. ElBakouri, D. W. Szczepanik, K. Jorner, R. Ayub, P. Bultinck, M. Solà, H. Ottosson, *J. Am. Chem. Soc.* **2022**, *144*, 8560–8575.

[14] a) M. O. Sandberg, O. Nagao, Z. Wu, M. M. Matsushita, T. Sugawara, *Chem. Commun.* **2008**, *32,* 3738−3740; b) K. P. Rao, T. Kusamoto, F. Toshimitsu, K. Inayoshi, S. Kume, R. Sakamoto, H. Nishihara, *J. Am. Chem. Soc.* **2010**, *132*, 12472−12479; c) X. Zheng, X. Wang, Y. Qiu, Y. Li, C. Zhou, Y. Sui, Y. Li, J. Ma, X. Wang, *J. Am. Chem. Soc.* **2013**,*135*, 14912−14915; d) X. Tao, C. G. Daniliuc, O. Janka, R. Pöttgen, R. Knitsch, M. R. Hansen, H. Eckert, M. Lübbesmeyer, A. Studer, G. Kehr, G. Erker, *Angew. Chem., Int. Ed.* **2017**, *56,* 16641−16644; *Angew. Chem.* **2017**, *129*, 16868–16871; e) X. Tao, C. G. Daniliuc, R. Knitsch, M.R. Hansen, H. Eckert, M. Lübbesmeyer, A. Studer, G. Kehr, G. Erker, *Chem. Sci.* **2018**, *9*, 8011−8018; f) L. Liu, L. L. Cao, Y. Shao, G. Ménard, D. W. Stephan, *Chem.* **2017**, *3*, 259−267; g) L. E. Longobardi, L. Liu, S. Grimme, D. W. Stephan, *J. Am. Chem. Soc.* **2016**,*138*, 2500−2503; h) S. X. Tang, L. Zhang, H. P. Ruan, Y. Zhao, X. P. Wang, *J. Am. Chem. Soc.* **2020**, *142*, 7340–7344; i) J. Wang, H. Y. Cui, H. P. Ruan, Y. Zhao, Y. Zhao, L. Zhang, X. P. Wang, *J. Am. Chem. Soc.* **2022**, *144*, 7978–7982; j) G. Tan, J. Li, L. Zhang, C. Chen, Y. Zhao, X. Wang , Y. Song , Y. Zhang, M. Driess, *Angew. Chem. Int. Ed.*, **2017**, *56*, 12741–12745; *Angew. Chem.* **2017**, *129*, 12915–12919.

[15] a) M. Stępień, E. Gońka, M. Żyła, N. Sprutta, *Chem. Rev.* **2017**, *117*, 3479–3716; b) X. Su, T. A. Bartholome, J. R. Tidwell, A. Pujol, S. Yruegas, J. J. Martinez, C. D. Martin, *Chem. Rev.* **2021**, *121*, 4147–4192; c) M. Hirai, N. Tanaka, M. Sakai, S. Yamaguchi, *Chem. Rev.* **2019,** *119*, 8291– 8331; d) K. Dhbaibi, L. Favereau, J. Crassous, *Chem. Rev.* **2019**, *119*, 8846–8953; e) X. Y. Wang, F. D. Zhuang, R. B. Wang, X. C. Wang, X. Y. Cao, J. Y. Wang, J. Pei, *J. Am. Chem. Soc.* **2014**, *136*, 3764 –3767; f) A. S. Scholz, J. G. Massoth, M. Bursch, J. M. Mewes, T. Hetzke, B. Wolf, M. Bolte, H. W. Lerner, S. Grimme, M. Wagner, *J. Am. Chem. Soc.* **2020**, *142*, 11072–11083; g) N. Ando, T. Yamada, H. Narita, N. N. Oehlmann, M. Wagner, S. Yamaguchi, *J. Am. Chem. Soc.* **2021**, *143*, 9944–9951; h) Y. Shi, Y. Zeng, P. Kucheryavy, X. Yin, K. Zhang, G. Meng, J. Chen, Q. Zhu, N. Wang, X. Zheng, F. Jäkle, P. Chen, *Angew. Chem., Int. Ed.* **2022**, *61*, e202213615; *Angew. Chem.* **2022**, *134*, e202213615; i) A. Borissov, Y. K. Maurya, L. Moshniaha, W. S. Wong, M. Żyła-Karwowska, M. Stępień, *Chem. Rev.* **2022**, *122*, 565–788; j) X. Y. Wang, X. Yao, A. Narita, K. Müllen, *Acc. Chem. Res.* **2019**, *52*, 2491–2505; k) X. Zhang, F. Rauch, J. Niedens, R. B. Silva, A. Friedrich, A. Nowak-Król, S. J. Garden, T. B. Marder, *J. Am. Chem. Soc.* **2022**, *144*, 22316–22324.

[16] a) L. Ji, S. Griesbeck, T. B. Marder, *Chem. Sci.* **2017**, *8*, 846–863; b) Vidal, F.; Jäkle, F. *Angew. Chem., Int. Ed.* **2019**, *58*, 5846–5870; *Angew. Chem.* **2019**, *131*, 5904–5929; c) Z. Huang, S. Wang, R. D. Dewhurst, N. V.; Finze, M. Ignat'ev, H. Braunschweig, *Angew. Chem., Int. Ed.* **2020,** *59*, 8800–8816; *Angew. Chem.* **2020**, *132*, 8882–8900; d) Y. Fu, H. Yang, Y. Gao, L. Huang, R. Berger, J. Liu, H. Lu, Z. Cheng, S. Du, H. J. Gao, X. Feng, *Angew. Chem., Int. Ed.* **2020**, *59*, 8873–8879; *Angew. Chem.* **2020**, *132*, 8958–8964; e) J. He, F. Rauch, M. Finze, T. B. Marder, *Chem. Sci.* **2021**, *12*, 128–147; f) J. Guo, Y. Yang, C. Dou, Y. Wang, *J. Am. Chem. Soc.* **2021**, *143*, 18272–18279; g) T. Fujikawa, Y. Segawa, K. Itami, *J. Am. Chem. Soc.* **2016**, *138*, 3587–3595; h) K. Xu, Y. Fu, Y. Zhou, F. Hennersdorf, P. Machata, I. Vincon, J. J. Weigand, A. A. Popov, R. Berger, X. Feng, *Angew. Chem. Int. Ed.* **2017**, *56*, 15876–15881; *Angew. Chem.* **2017**, *129*, 16092–16097.

[17] a) J. F. Chen, X. Yin, B. Wang, K. Zhang, G. Meng, S. Zhang, Y. Shi, N. Wang, S. Wang, P. Chen, *Angew. Chem., Int. Ed.* **2020**, *59*, 11267–11272; *Angew. Chem.* **2020**, *132*, 11363–11368; b) F. Zhao, J. Zhao, Y. Wang, H. T. Liu, Q. Shang, N. Wang, X. Yin, X. Zheng, P. Chen, *Dalton Trans.* **2022**, *51*, 6226–6234; c) K. Zhang, J. Zhao, N. Zhang, J. F. Chen, N. Wang, X. Yin, X. Zheng, P. Chen, *J. Mater. Chem. C.* **2022**, *10*, 1816–1824; d) H. W. Li, M. Li, Z. H. Zhao, C. F. Chen, Q. Peng, C. H. Zhao, *Org. Lett.* **2021**, *23*, 4759–4763; e) M. Y. Zhang, X. Liang, D. N. Ni, D. H. Liu, Q. Peng, C. H. Zhao, *Org. Lett.* **2021**, *23*, 2–7; f) M. Y. Zhang, Z. Y. Li, B. Lu, Y. Wang, Y. D. Ma, C. H. Zhao, *Org. Lett.* **2018**, *20*, 6868–6871.

[18] a) Z. H. Zhao, X. Liang, M. X. He, M. Y. Zhang, C. H. Zhao, *Org. Lett.* **2019**, *21*, 9569–9573; b) Z. B. Sun, J. K. Liu, D. F. Yuan, Z. H. Zhao, X. Z. Zhu, D. H. Liu, Q. Peng, C. H. Zhao, *Angew. Chem., Int. Ed.* **2019**, *58*, 4840–4846; *Angew. Chem.* **2019**, *131*, 4894–4900; c) J. Full, S. P. Panchal, J. Götz, A. M. Krause, A. Nowak-Król, *Angew. Chem., Int. Ed.* **2021**, *60*, 4350–4357; *Angew. Chem.* **2021**, *133*, 4396–4403; d) J. K. Li, X. Y Chen, Y. L. Guo, X. C. Wang, A. C. H. Sue, X. Y. Cao, X. Y. Wang, *J. Am. Chem. Soc.* **2021**, *143*, 17958–17963; e) J. Dosso, B. Bartolomei, N. Demitri, F. P. Cossío, M. Prato, *J. Am. Chem. Soc.* **2022**, *144*, 7295–7301; f) S. Kasemthavee-chok, L. Abella, M. Jean, M. Cordier, T. Roisnel, N. Vanthuyne, T. Guizouarn, O. Cador, J. Autschbach, J. Crassous, L. Favereau, *J. Am. Chem. Soc*. **2020**, *142*, 20409–20418; g) S. Kasemthaveechok, L. Abella, M. Jean, M. Cordier, N. Vanthuyne, T. Guizouarn, O. Cador, J. Autschbach, J. Crassous, L. Favereau, *J. Am. Chem. Soc.* **2022**, *144*, 7253–7263; h) H. Sato, R. Suizu, T. Kato, A. Yagi, Y. Segawa, K. Awaga, K. Itami, *Chem. Sci.* **2022**, *13*, 9947–9951; i) H. Wei, X. Hou, T. Xu, Y. Zou, G. Li, S. Wu, Y. Geng, J. Wu, *Angew. Chem. Int. Ed.* **2022**, *61*, e202210386; *Angew. Chem.* **2022**, *134*, e202210386.

[19] a) X. Gu, T. Y. Gopalakrishna, H. Phan, Y. Ni, T. S. Herng, J. Ding, J. Wu, *Angew. Chem. Int. Ed.*, **2017**, *48*, 15383–15387; *Angew. Chem.* **2017**, *122*, 5591–5594; b) Y. Ni, F. Gordillo-Gámez, M. Peña Alvarez, Z. Nan, Z. Li, S. Wu, Y. Han, J. Casado and J. Wu, *J. Am. Chem. Soc.* **2020**, *142,* 12730–12742; c) S. Wu, Yong Ni, Yi Han, X. Hou, C. Wang, W.

Hu, J. Wu, *Angew. Chem. Int. Ed.,* **2021**, *61*, e202115571; *Angew. Chem.* **2021**, *134*, e202115571; d) L. Ren, Y. Han, X. Hou, Y. Ni, J. Wu, *Chem*., **2021**, *7*, 3442–3453; e) S. Wu, Y. Ni, Y. Han, S. Xin, X. Hou, J. Zhu, Z. Li, J. Wu, *J. Am. Chem. Soc.* **2022**, *144*, 23158–23167; f) Y. Ni, T. Y. Gopalakrishna, H. Phan, T. Kim , T. S. Herng, Y. Han, T. Tao, J. Ding, D. Kim, J. Wu, *Nature Chemistry.*, **2020**, *12*, 242–248; g) T. Fujiwara, A. Muranaka, T. Nishinaga, S. Aoyagi, N. Kobayashi, M. Uchiyama, H. Otani, M. Iyoda, *J. Am. Chem. Soc.* **2020**, *142,* 5933–5937.

[20] a) H. Han, Y. Huang, C. Tang, Y. Liu, M. D. Krzyaniak, B. Song, X. Li, G. Wu, Y. Wu, R. Zhang, Y. Jiao, X. Zhao, X. Chen, H. Wu, C. L. Stern, Y. Ma, Y. Qiu, M. R. Wasielewski, J. F. Stoddart, *J. Am. Chem. Soc.* **2023**, *145*, 18402–18413; b) J. Fujita, M. Tanaka, H. Suemune, N. Koga, K. Matsuda, H. Iwamura, *J. Am. Chem. Soc.* **1996**, *118*, 9347−9351; c) D. A. Shultz, R. K. Kumar, *J. Am. Chem. Soc.* **2001**,*123*, 6431−6432; d) T. Ise, D. Shiomi, K. Sato, T. Takui, *Chem. Mater.* **2005**, *17*, 4486−4492; e) V. Lloveras, E. Badetti, K. Wurst, J. Vidal-Gancedo, *Chem Phys Chem.* **2015**, *16*, 3302−3307; f) R. Kurata, D. Sakamaki, M. Uebe, M. Kinoshita, T. Iwanaga, T. Matsumoto, A. Ito, *Org. Lett.* **2017**,*19*, 4371−4374; g) Y. Hattori, E. Michail, A. Schmiedel, M. Moos, M. Holzapfel, I. Krummenacher, H. Braunschweig, U. Müller, J. Pflaum, C. Lambert, *Chem. Eur. J.* **2019**, *25*, 15463−15471; h) X. Dong, Q. C. Luo, Y. Zhao, T. Wang, Q.C. Sun, R.B. Pei, Y. Zhao, Y.Z. Zheng, X. P. Wang, *J. Am. Chem. Soc.,* **2023**, *145*, 17292–17298, and references therein.

[21] C. Li, C. Zhang, P. Li, Y. Jia, J. Duan, M. Liu, N. Zhang, P. Chen, *Angew. Chem. Int. Ed.,* **2023**, *62*, e202302019; *Angew. Chem.* **2023**, *135*, e202302019.

[22] F. Zhao, J. Zhao, H. Liu, Y. Wang, J. X. Duan, C. L. Li, J. Q. Di, N. Zhang, X. Y. Zheng, P. K. Chen. *J. Am. Chem. Soc.,* **2023**, *145*, 10092–10103.

[23] We thank one of the reviewers for the suggestion on analysis of diradical dication **$1^{2+2\bullet+}$2SbF$_6^-$**. We note that upon the addition of $NOSbF_6$ the reaction system may consist of more than one cationic species due to the consecutive oxidations of carbazole units in the cyclic structure of **1**, leading to the difficulty in clearly identifying the obtained components based on experiments. However, an alternative approach can be employed to predict the formation of dominant diradical dications as we tried to match the computational UV-vis-NIR absorption profiles with the experimentally observed absorptions (see Figure 3 and Figure 5a).

[24] a) H. Gao, X. Zhi, F. Wu, Y. Zhao, F. J. Cai, P. F. Li, Z. Shen, *Angew. Chem. Int. Ed.* **2023**, *62*, e202309208; *Angew. Chem.* **2023**, *135*, e202309208; b) B. Lü, Y. Chen, P. Li, B. Wang, K. Müllen, M. Yin, *Nat. Commun.* **2019**, *10*, 767; c) H. Wang, K. F. Xue, Y. Yang, H. Hu, J. F. Xu, X. Zhang, *J. Am. Chem. Soc.* **2022**, *144*, 2360–2367; d) S. Park, J. Lee, H. Jeong, S. Bae, J. Kang, D. Moon, J. Park, *Chem.* **2022**, *8*, 1993–2010; e) J. Su, N. Xu, R. Murase, Z. M. Yang, D. M. D'Alessandro, J. L. Zuo, J. Zhu, *Angew. Chem. Int. Ed.* **2021**, *60*, 4789–4795; *Angew. Chem.* **2021**, *133*, 4839-4845; f) T. Yan, Y. Y. Li, J. Su, H. Y. Wang, J. L. Zuo, *Chem. Eur. J.* **2021**, *27*, 11050–11055; g) Z. Mi, P. Yang, R. Wang, J. Unruangsri, W. Yang, C. Wang, J. Guo, *J. Am. Chem. Soc.* **2019**, *141*, 14433–14442; h) B. Tang, W. L. Li, Y. Chang, B. Yuan, Y. Wu, M. T. Zhang, J. F. Xu, J. Li, X. Zhang, *Angew. Chem. Int. Ed.* **2019**, *58*, 15526–15531; *Angew. Chem.* **2019**, *131*, 15672–15677; i) X. Cui, G. Lu, S. Dong, S. Li, Y. Xiao, J. Zhang, Y. Liu, X. Meng, F. Li, C. S. Lee, *Mater. Horiz.* **2021**, *8*, 571–576.

[25] L. Arrico, L. Di Bari, F. Zinna, *Chem.-Eur. J.* **2021**, *27*, 2920–2934.

[26] Deposition number 2264701 (for **N7H2Br**) contains the supplementary crystallographic data for this paper. These data are provided free of charge by the joint Cambridge Crystallographic Data Centre and Fachinformationszentrum Karlsruhe Access Structures service.

10.1002/ange.202402800

WILEY-VCH

RESEARCH ARTICLE

Entry for the Table of Contents

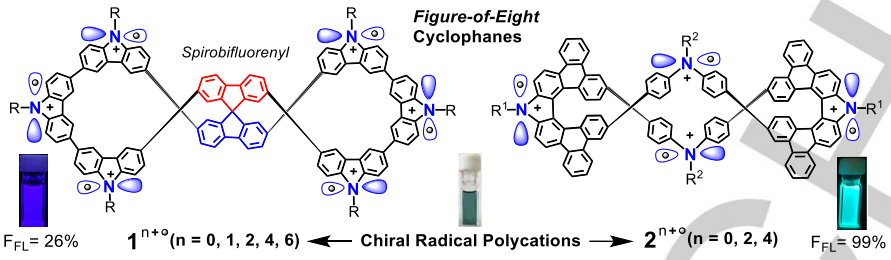

π-conjugated new chiral macrocycles **1** and **2** have been accessed using the redox-active main-group carbazole and *π*-expanded aza[7]helicene moieties. Chemical and electrochemical oxidations of these electron-rich figure-of-eight macrocycles readily enabled the conversion to chiral polycationic open-shell cyclophanes with tunable electronic states that are rarely accessible from the all-carbon-based analogues.

Institute and/or researcher Twitter usernames: ((optional))